TOPOLOGICAL GRADIENT FOR A FOURTH ORDER PDE AND APPLICATION TO THE DETECTION OF FINE STRUCTURES IN 2D AND 3D IMAGES

Audric Drogoul, Gilles Aubert, Didier Auroux

Université de Nice Sophia Antipolis, CNRS, LJAD, UMR 7351, 06100 Nice, France

ABSTRACT

In this paper we describe a new variationnal approach for the detection of fine structures in an image (like filaments in 2D). This approach is based on the computation of the topological gradient associated to a cost function defined from the second derivatives of a regularization of the data (possibly noisy and / or blurred). We get this approximation by solving a fourth order PDE. The study of the topological sensitivity is made in the case of a crack. We give the numerical algorithm to compute this topological gradient and we illustrate our approach by giving several experimental results in 2D and 3D images.

Index Terms— Object detection, Fine structures, Image segmentation, Calculus of variations, Topological Gradient

1. INTRODUCTION

In image processing, segmentation / restoration or detection of fine structures are challenging problems with many applications (in satellite, medical, biological imaging etc ...). In this work we give and experiment a variational model to detect fine structures (filaments and points in 2D, surfaces and filaments in 3D) by using the topological gradient method. First introduced by Sokolowski [1] and Masmoudi [2], this notion consists in the study of the variations of a cost function $j(\Omega) = J_\Omega(u_\Omega)$ with respect to a topological variation where $J_\Omega(u)$ is of the form $J_\Omega(u) = \int_\Omega F(u, \nabla u, \nabla^2 u, ...)$; u_Ω is a solution of a PDE defined on the image domain Ω. To calculate the topological gradient we remove to Ω an object ω_ϵ of size $\epsilon \to 0$ centered to x_0 (generally a ball or a crack) and we calculate the limit $\mathcal{I}(x_0) = \lim_{\epsilon\to 0} \frac{j(\Omega\setminus\overline{\omega_\epsilon}) - j(\Omega)}{\epsilon^d}$ where d is the dimension of the ambiant space. $\mathcal{I}(x_0)$ is called the topological gradient at x_0. A particularity of this method is that the computation of the topological gradient only needs the direct state u_Ω and an adjoint state v_Ω solution of a similar PDE depending on u_Ω. This makes the topological gradient computation easy and very fast. Initially used in mechanic of structures, this method has been used in image processing by several authors. For example by Belaid etal. in [3] in restoration / segmentation problems. In this case $F(\nabla u) = |\nabla u|^2$ and u_Ω is the solution of a Laplace PDE. The focus of the method is to find points which contain the most of energy and associated to a high topological gradients. If for edges detection the use of the gradient operator for the cost function is classical, it is known [4] that this choice is not adapted for filaments detection : the "gradient does not see " these structures. To illustrate this fact let us consider in 1D the function $f(x) = 0$ if $x \neq 0$ and $f(0) = 1$. This function can be approximated by the function $f_\eta(x) = 0$ if $|x| \geq \eta$ and $f_\eta(x) = \frac{2}{\eta^3}|x|^3 - \frac{3}{\eta^2}|x|^2 + 1$ if $|x| \leq \eta$. We have $f'_\eta(0) = 0$ but $f''_\eta(0) = \frac{-6}{\eta^2}$, thus f'_η "does not see" 0 but f''_η becomes singular at 0. Other variationnal models have been proposed in the literature according to applications, see [5] for the detection of biological filaments or [6] for road network detection. In [7] authors propose a model for detecting objects of codimension two and one in 2D images. Their method is inspired by Ginzburg-Landau models. There exists of course other approaches not based on variational calculus. In [8] a morphological method is presented ; authors use morphological filters and a curvature evaluation to detect vessel-like patterns. In [9] a thin network is simulated by a point process which penalizes not connected segments and favors aligned segments. The estimate of the network is obtained by minimising an energy function. Finally let us mention the wavelet approach [10].
In this paper we present a new variational model based on the topological gradient method inspired from the static PDE of a deflection of a thin plate subject to transverse force and bending moment. In this case $F(\nabla^2 u) = \|\nabla^2 u\|^2$ and u_Ω is the solution of a PDE based on the Bilaplacian operator. The model presented here allows to detect filaments and points in 2D images (surfaces and filaments in 3D images) blurred and / or noisy by Gaussian noise. The paper is organized as follows. In section 2 we present the problem and give the main idea to compute the topological gradient (TG) in the case of a crack. In section 3, we develope the numerical algorithm for computing the TG and give some numerical results in 2D and 3D.

Contact: drogoula@unice.fr, gaubert@unice.fr, auroux@unice.fr

2. PROBLEM STATEMENTS AND COMPUTATION OF THE TOPOLOGICAL GRADIENT

2.1. Problem statement

We suppose that the observed image f writes as $f = Ku + n$ where K is a blurring operator, n a Gaussian noise and u the image to recover. We introduce the cost function and the PDE introduced in [11]. The model is inspired by the Kirchhoff thin static plate model subject to pure bending (see [12]) with a Poisson ratio $\nu = 0$. We denote $J_\epsilon(u) = J_{\Omega_\epsilon}(u)$ the cost function defined by:

$$J_\epsilon(u) = \int_{\Omega_\epsilon} \|\nabla^2 u\|^2, \tag{1}$$

where for a matrix M we denote $\|M\|^2 = tr(M^T M)$. Let $u_\epsilon = u_{\Omega_\epsilon}$ be a regularization of the observed image $f \in L^2(\Omega_\epsilon)$ solution of the following minimization problem :

$$\min_{u \in H(\Omega_\epsilon)} \left(\alpha J_\epsilon(u) + \|Ku - f\|^2_{L^2(\Omega_\epsilon)} \right) \qquad (\mathcal{P}_\epsilon) \tag{2}$$

where $\alpha > 0$ is a parameter that we have to tune and $H(\Omega_\epsilon) = \left\{ u \in L^2(\Omega_\epsilon), \nabla^2 u_\epsilon \in L^2(\Omega_\epsilon) \right\}$ and $K : L^2(\Omega_\epsilon) \to L^2(\Omega_\epsilon)$ is a linear operator.
The variational formulation of $(\mathcal{P}_\epsilon)$ writes as:

$$\text{find } u_\epsilon \in H(\Omega_\epsilon) : a_\epsilon(u_\epsilon, v) = l_\epsilon(v),\ \forall v \in H(\Omega_\epsilon) \tag{3}$$

where $a_\epsilon(u, v)$ and $l_\epsilon(v)$ denote the following bilinear and linear forms:

$$\begin{aligned} a_\epsilon(u, v) &= \int_{\Omega_\epsilon} \alpha \sum_{1 \le i,j \le 2} \frac{\partial^2 u}{\partial x_i \partial x_j} \frac{\partial^2 v}{\partial x_i \partial x_j} + KuKv \\ l_\epsilon(v) &= \int_{\Omega_\epsilon} K^\star f v. \end{aligned} \tag{4}$$

where $K^\star$ denotes the adjoint operator of K. The Euler equations associated with $(\mathcal{P}_\epsilon)$ are

$$(\mathcal{P}_\epsilon) \begin{cases} \alpha \Delta^2 u_\epsilon + K^\star K u_\epsilon = K^\star f, \text{ on } \Omega_\epsilon \\ B_1 u_\epsilon = B_2 u_\epsilon = 0, \text{ on } \partial\Omega_\epsilon \end{cases} \tag{5}$$

where

$$\begin{aligned} B_1 u &= \partial_n(\Delta u) - \partial_\sigma \left(n_1 n_2 \left(\frac{\partial^2 u}{\partial x_1^2} - \frac{\partial^2 u}{\partial x_2^2} \right) \right. \\ &\quad \left. -(n_1^2 - n_2^2) \frac{\partial^2 u}{\partial x_1 \partial x_2} \right) \\ B_2 u &= n_1^2 \frac{\partial^2 u}{\partial x_1^2} + n_2^2 \frac{\partial^2 u}{\partial x_2^2} + 2 n_1 n_2 \frac{\partial^2 u}{\partial x_1 \partial x_2} \end{aligned}$$

setting $\vec{n} = (n_1, n_2)$ the outer normal to the domain, and $\vec{\sigma} = (\sigma_1, \sigma_2)$ the tangent vector such that $(\vec{n}, \vec{\sigma})$ forms an orthonormal basis.
In mechanics $B_1(u)$ is the transverse force (shear force and twisting moment), $B_2(u)$ represents the bending moment and u is the deflection of the thin plate.

2.2. Computation of the topological gradient in 2D

The calculus of the topological gradient is very technical. In this section we just give the important steps and the main ideas in the case of the crack with $\alpha = 1$ and $K = I_d$.
Notations. To simplify, we suppose that the crack is centered at 0 and writes as $\sigma = \{(s, 0), -1 < s < 1\}$. We denote by $\widetilde{\sigma}$ a fixed smooth closed curve that contains σ and by $\widetilde{\omega}$ the set such that $\partial\widetilde{\omega} = \widetilde{\sigma}$. For $x \in \sigma$, u^+ and u^- denotes the limit values $\lim_{y \to x, y \in \widetilde{\omega}^c} u(y)$ and $\lim_{y \to x, y \in \widetilde{\omega}} u(y)$ and $[u] = u^+ - u^-$ the jump across σ. We set $\sigma_\epsilon = \left\{ x, \frac{x}{\epsilon} \in \sigma \right\}$, Λ the exterior space $\mathbb{R}^2 \backslash \overline{\sigma}$ and Ω_ϵ the cracked domain $\Omega \backslash \overline{\sigma_\epsilon}$.

Main ideas. In order to evaluate the leading term in the difference $J_\epsilon(u_\epsilon) - J_0(u_0)$ we introduce an *adjoint problem* $v_\epsilon \in H(\Omega_\epsilon)$ solution of :

$$a_\epsilon(u, v_\epsilon) = -L_\epsilon(u), \forall u \in H(\Omega_\epsilon) \tag{6}$$

with $L_\epsilon(u) = \int_{\Omega_\epsilon} K^\star(f - 2Ku_0)u$. Then by integration by parts we get

$$J_\epsilon(u_\epsilon) - J_0(u_0) = \int_{\sigma_\epsilon} B_1 u_0 [w_\epsilon] - B_2 u_0 [\partial_n w_\epsilon] - A_\epsilon \tag{7}$$

with $w_\epsilon = v_\epsilon - v_0$, $A_\epsilon = \|u_\epsilon - u_0\|^2_{L^2(\Omega_\epsilon)}$ and where $[w_\epsilon]$ and $[\partial_n w_\epsilon]$ denote the jumps across σ_ϵ of w_ϵ and $\partial_n w_\epsilon$. Next we approximate w_ϵ by $w_\epsilon = \epsilon^2 P\left(\frac{x}{\epsilon}\right) + e_\epsilon$ where $e_\epsilon \in H(\Omega_\epsilon)$ and $\|e_\epsilon\|_{H(\Omega_\epsilon)} = O(\epsilon^2 log(\epsilon))$ and where $P \in W^2(\Lambda)/\mathbb{P}_1$ is the *exterior problem* defined by

$$(\mathcal{P}_{ext}) \begin{cases} \Delta^2 P = 0, \text{ on } \Lambda \\ B_1 P = 0, \text{ and } B_2 P = V_2 \text{ on } \sigma \end{cases} \tag{8}$$

where $V_2 = -\frac{\partial^2 v_0}{\partial x_2^2}(0)$ is such that $B_2(v_0)(x) = V_2 + O(\epsilon)$. We recall that $W^2(\Lambda)/\mathbb{P}_1$ is the weighted sobolev space functions defined up to the polynomial functions of degree less or equal to one. We know [11] that P writes as a *multilayer potential* :

$$P(x) = \oint_\sigma \lambda_1(y) B_{1,y} E(x-y) d\sigma_y + \oint_\sigma \lambda_2(y) B_{2,y} E(x-y) d\sigma_y$$

where $\oint$ denotes the principal Cauchy value and $E(x)$ is the fundamental solution associated to the Bilaplacian operator. We can show that $[P] = \lambda_1 = 0$ and $[\partial_n P(x)] = \lambda_2(x) = \frac{4}{3} V_2 \sqrt{1 - x_1^2}$. Thus (7) expresses as

$$J_\epsilon(u_\epsilon) - J_0(u_0) = -\frac{2\pi}{3} \epsilon^2 \frac{\partial^2 u_0}{\partial x_2^2}(0) \frac{\partial^2 v_0}{\partial x_2^2}(0) + o(\epsilon^2)$$

2.3. Expression of the topological gradient in the general case in 2D

The topological gradient of the function $\epsilon \mapsto J_\epsilon(u_\epsilon)$ whith u_ϵ given by (3) and for a crack centered at x_0 and of normal $\vec{n}$ is

[11] :

$$\mathcal{I}(x_0,\vec{n}) = -\frac{2\pi}{3}\alpha\nabla^2 u_0(x_0)(\vec{n},\vec{n})\nabla^2 v_0(x_0)(\vec{n},\vec{n}) \quad (9)$$

where u_0 and v_0 are respectively given by (5) and (6) with $\epsilon = 0$. The topological gradient at point x_0 is obtained from (9) by taking the max of its absolute value over $\vec{n}$:

$$\mathcal{I}(x_0) = \max_{\|\vec{n}\|=1} |\mathcal{I}(x_0,\vec{n})| \quad (10)$$

Remark 2.1 *In 3D we can model a planar circular crack by* $\sigma = \{(rcos(\theta), rsin(\theta), 0),\ 0 \leq r < 1, 0 \leq \theta < 2\pi\}$, *and by similar calculus we have the TG expression :*

$$\mathcal{J}(x_0,\vec{n}) = -\frac{4\pi}{3}\alpha\nabla^2 u_0(x_0)(\vec{n},\vec{n})\nabla^2 v_0(x_0)(\vec{n},\vec{n}) \quad (11)$$

Remark 2.2 *We will check numerically that the maximum magnitude of* $\mathcal{I}(x_0)$ *is reached when* $\vec{n}$ *is perpendicular to the filament direction.*

3. NUMERICAL ALGORITHM AND EXPERIMENTAL RESULTS

In this section we describe the numerical method to perform the TG (10) and give some experiment results.

3.1. Algorithm

To compute the TG given in (10) we need to compute the solution u_0 and v_0 given by (3) and (6) for $\epsilon = 0$. To do that we consider that Ω is the unit square and we extend f by symmetry with respect to the boundary of Ω and by periodicity. Then we can perform u_0 and v_0 by DCT (Discret Cosine Transform). The computation time is a $\mathcal{O}(Nlog(N))$ where N denotes the number of pixels (or voxels). If we represent the blur K by a convolution operator we get the solutions in the Fourier domain :

$$\widehat{u_0} = \frac{\widehat{K^\star}\hat{f}}{\alpha|\nu|^4 + \widehat{K^\star}\widehat{K}} \qquad \widehat{v_0} = \frac{2\widehat{K^\star}\widehat{K}\widehat{u_0} - \widehat{K^\star}\widehat{f}}{\alpha|\nu|^4 + \widehat{K^\star}\widehat{K}} \quad (12)$$

where ν is the discrete Fourier variable and $\widehat{K}$, $\widehat{K^\star}$, $\widehat{f}$, $\widehat{u_0}$ and $\widehat{v_0}$ the array of Fourier coefficients. The discrete solutions u_0 and v_0 are then obtained from (12) by using the IDCT (Inverse DCT). We compute the Hessian matrices $\nabla^2 u_0$ and $\nabla^2 v_0$ at each point of the meshgrid by convolution with derivative filters; finally we approximate (10) by writting $\vec{n}$ in polar or spherical coordinates and by taking the discrete maximum. All calculus are implemented in Matlab 7.5.0 and the experiments are performed on a computer equipped with a processor Intel Core 1.9 GHz.

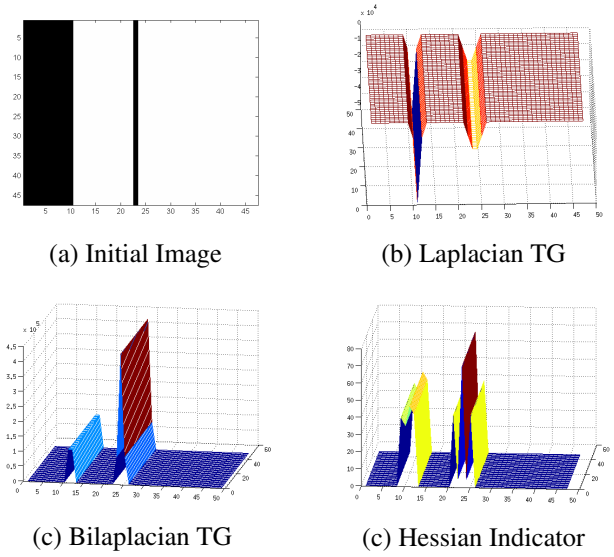

(a) Initial Image (b) Laplacian TG

(c) Bilaplacian TG (c) Hessian Indicator

Fig. 1. Comparsion of the TG I_{Bilap} (with $\alpha = 10^{-4}$) with the indicators I_{Lap} (with $\alpha = 10^2$) and I_{Hes} (with $\sigma = 5/4$) on a simple not noisy image

3.2. Experimental results in 2D

In this section we will compare the TG with an indicator based on the Hessian matrix eigenvalues of a Gaussian convolution of the image and used in [4]. We will denote by I_{Hes} this indicator. Figure 1 displays an image containing both an edge and a filament. The TG given in [3] associated to $F(u) = |\nabla u|^2$ is denoted I_{Lap}, the TG performed in (10) I_{Bilap}. First we see that I_{Lap} detects more the edge than the filament while I_{Bilap} (and also the Hessian indicator but less clearly) detects more the filament than the edge. In Figure 2 we display both I_{Hes} and I_{Bilap} for a very noisy image containing a filament, and we see that I_{Hes} is less robust with respect to the noise than the TG I_{Bilap}. Figure 3 displays the TG I_{Bilap} and the indicator I_{Hes} for a blurred and noisy image. The result is clear : I_{Hes} is inefficient in this case while the TG always detects the filament. The dimension of images are : 49×49 for Figure 1, 132×112 for Figure 2 and 193×165 for Figure 3. The computation times for Figures 1,2 and 3 are about 0.2 sec.

3.3. Experimental results in 3D

Here we illustrate the fact that the method can be easily extended to 3D imaging with the TG (11). The DCT is again used and the computation of the TG is very fast (for $N = 3.6 \times 10^5$: 0.22 sec for computing u_0, v_0 $\nabla^2 u_0$ and $\nabla^2 v_0$ and 25 sec to compute (10)). On Figure 4 we display the TG on 3D noisy images containing a filament (cylinder of length 3 voxels) and spheres. The visualisation is made by isosurface and we see that the topological gradient is quite smooth.

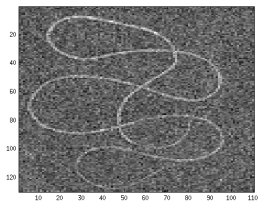

(a) Initial Image

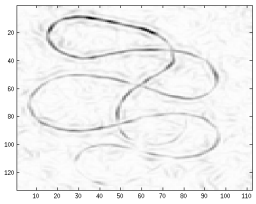

(b) TG

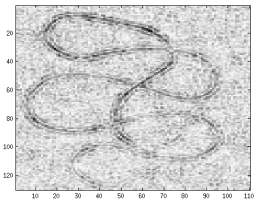

(c) Hessian Indicator

Fig. 2. Comparison of the TG (with $\alpha = 0.5$) with the indicator I_{Hes} (with $\sigma = 7/4$) on a noisy image (PSNR=14dB)

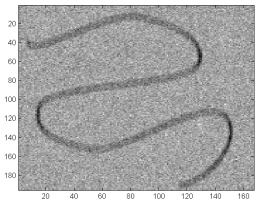

(a) Initial Image

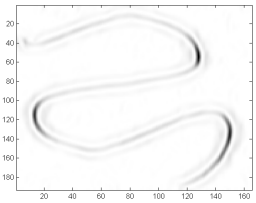

(b) TG

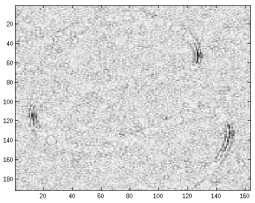

(b) TG

Fig. 3. Comparison between the TG ($\alpha = 5 \times 10^{-3}$) with the indicator I_{Hes} ($\sigma = 5/4$) on a motion blurred ($\theta = 90^o$, len=7) and Gaussian noised image (PSNR=16dB)

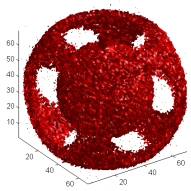

(a_1) Initial Image

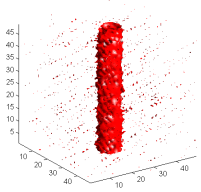

(a_2) Initial Image

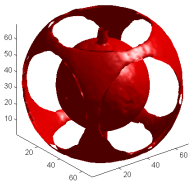

(b_1) TG

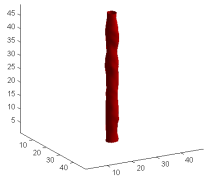

(b_2) TG

Fig. 4. Images and Topological gradients for Gaussian noisy images (PSNR=16dB), top : noisy images, bottom : T.G

.

4. CONCLUSION

In this paper we have proposed a new detector (the topological gradient) of fine structures in 2D or 3D imaging. The main qualities of this detector is its simplicity and rapidity. Moreover it is quite efficient and robust both in the case of noisy and blurred images.

.

5. REFERENCES

[1] J. Sokolowski and A. Zochowski, "On the topological derivative in shape optimization," *SIAM J. Control Optim.*, vol. 37, no. 4, pp. 1251–1272, Apr. 1999.

[2] M. Masmoudi, "The topological asymptotic," *Computational Methods for Control Applications*, vol. 16, 2001.

[3] D. Auroux, M. Masmoudi, and L. Jaafar Belaid, *Image restoration and classification by topological asymptotic expansion*, pp. 23–42, Variational Formulations in Mechanics: Theory and Applications, E. Taroco, E.A. de Souza Neto and A.A. Novotny (Eds). CIMNE, Barcelona, Spain, 2007.

[4] C. Steger, "An unbiased detector of curvilinear structures," *IEEE Trans. Pattern Anal. Mach. Intell.*, vol. 20, no. 2, pp. 113–125, 1998.

[5] M. Jacob and T. Blu and C. Vaillant and J.H. Maddocks and M. Unser, "3D shape estimation of DNA molecules from stereo cryo-electron micro-graphs using a projection-steerable snake," *IEEE Trans. Image Process*, vol. 15, pp. 214–227, 2006.

[6] M. Rochery, I.H. Jermyn, and J. Zerubia, "New higher-order active contour energies for network extraction.," in *ICIP (2)*. 2005, pp. 822–825, IEEE.

[7] A. Baudour, G. Aubert, and L. Blanc-Féraud, "Detection and Completion of Filaments: A Vector Field and PDE Approach.," in *SSVM*, Fiorella Sgallari, Almerico Murli, and Nikos Paragios, Eds., 2007, vol. 4485 of *Lecture Notes in Computer Science*, pp. 451–460.

[8] F. Zana and J-C. Klein, "Segmentation of vessel-like patterns using mathematical morphology and curvature evaluation.," *IEEE Transactions on Image Processing*, vol. 10, no. 7, pp. 1010–1019, 2001.

[9] R. Stoica, X. Descombes, and J. Zerubia, "A Gibbs Point Process for Road Extraction from Remotely Sensed Images.," *International Journal of Computer Vision*, vol. 57, no. 2, pp. 121–136, 2004.

[10] KM. Liew and Q. Wang, "Application of wavelet theory for crack identification in structures.," *Journal of Engineering Mechanics*, vol. 124, no. 2, pp. 152–157, 1998.

[11] G. Aubert and A. Drogoul, "A topological gradient based model for the detection of fine structures in 2D images (submitted)," .

[12] J. Zhou G. Chen, *Boundary Element Methods with Applications to Nonlinear Problems*, Artlantis studies in Mathematics for Engineering and Science, 1992.